Frequency Effects in Pol-InSAR Forest Height Estimation.

Florian Kugler[1], Fifame N. Koudogbo[1], Karlheinz, Gutjahr[2] & Konstantinos P. Papathanassiou[1]
1- German Aerospace Center (DLR), Microwaves and Radar Institute Germany
2- Joanneum Research, Institute for Digital Image Processing Graz, Austria

Abstract

Forest height has been related and inverted from interferometric measurements at different baselines, polarisations, frequencies. In this paper the effect of frequency on model based inversion of forest height from interferometric measurements is addressed and obtained experimental results at X, L and P Band are discussed.

1 Introduction

Synthetic Aperture Radar Interferometry (InSAR) generated a great deal of interest in forest remote sensing applications. Recent experiments [1, 2] demonstrated the model based inversion of forest height from polarimetric interferometric SAR (Pol-InSAR) data at L Band for a variety of forest and terrain conditions. Apart of the importance of forest height as single forest parameter, the inherent relation between forest height and forest biomass, manifested by general allometric relations makes forest height inversion from SAR interferometry a topic of actual importance. In this paper the impact of frequency on the inversion of forest height is discussed and demonstrated using experimental X, L, and P Band data acquired by DLR's E-SAR system over the Kobernausser Wald test site in Austria.

2 Volume Coherence

The (complex) volume decorrelation contribution $\tilde{\gamma}_V$ of the interferometric coherence is directly related to the normalised Fourier transformation of the vertical distribution of scatterers *F(z)* [3]

$$\tilde{\gamma}_V = exp(i\kappa_z z_0)\frac{\int_0^{h_V} F(z')exp(i\kappa_z z')dz'}{\int_0^{h_V} F(z')dz'} \qquad -1)$$

where κ_z is the effective vertical interferometric wavenumber that depends on the imaging geometry and the radar wavelength

$$\kappa_z = \frac{\kappa\Delta\theta}{sin(\theta_0)} \quad \text{and} \quad \kappa = \frac{4\pi}{\lambda} \qquad -2)$$

and $\Delta\theta$ is the incidence angle difference between the two interferometric images induced by the baseline. z_0 is a reference height. In this context the estimation of vertical forest structure parameters from interferometric measurements can be addressed as a two step process: In the first step (modeling) *F(z)* is parameterized in terms of a more or less limited set of physical forest parameters that are related through Eq. 1 to the interferometric coherence. In the second step (inversion), the volume contribution of the measured interferometric coherence is then used to estimate *F(z)* and to derive the corresponding parameters. In the following the most common approaches to model *F(z)* will be reviewed.

In the simplest case, *F(z)* accounts only for the vertical extension of the scatterers assuming a homogeneous distribution of scatterers

$$F(z) = ct \quad \text{with} \quad z_0 \le z \le z_0 + h_V \qquad -3)$$

Eq. 3 leads to the characteristic sinc-decorrelation function that depends on a single parameter namely the volume height h_V

$$\tilde{\gamma}_V = exp(i\kappa_z z_0)exp(i\frac{\kappa_z h_V}{2})sinc(\frac{\kappa_z h_V}{2}) \qquad -4)$$

where *sinc(x)=sin(x)/x.* A more realistic modelisation of *F(z)* accounts for the attenuation of the wave through the volume in terms of a mean extinction coefficient σ (that is a function of the density of the scatterers in the volume and their dielectric constant)

$$F(z) = exp\left(\frac{2\sigma}{sin(\theta_0)}z\right) \qquad -5)$$

Eq. 5 leads to the so called random volume (RV) formulation [4]

$$\tilde{\gamma}_V = exp(i\kappa_z z_0)\frac{\int_0^{h_V} exp(i\kappa_z z')exp\left(\frac{2\ \sigma\ z'}{cos\theta_0}\right)dz'}{\int_0^{h_V} exp\left(\frac{2\ \sigma\ z'}{cos\theta_0}\right)dz'} \qquad -6)$$

The introduction of an impenetrable layer on the bottom of the volume (i.e., $z:=z_0$) – in order to account for any ground scattering component characterised by

an isolated phase center in height (i.e., direct ground and/or dihedral scattering)

$$F(z) = \tilde{m}_V \exp\left(\frac{2\sigma}{\sin(\theta_0)} z\right) + m_G \delta(z - z_0) \qquad -7)$$

leads to the Random Volume over Ground (RvoG) model formulation [5]

$$\tilde{\gamma}_V = \exp(i\kappa_z z_0) \frac{\tilde{\gamma}_{V0} + m}{1 + m} \qquad -8)$$

$\varphi_0 = \kappa_z z_0$ is now the phase related to the ground topography z_0 and m the effective ground-to-volume amplitude ratio accounting for the attenuation through the volume:

$$m = \frac{m_G}{m_V I_0} \qquad -9)$$

$\tilde{\gamma}_{V0}$ is the volume decorrelation caused in the absence of the ground layer and corresponds to Eq. 6. As next the polarization and frequency dependency of *F(z)* will be discussed.

2.1 Polarisation Dependency

According to Eq. 1, when the vertical distribution of scatterers *F(z)* changes with polarisation then the interferometric coherence varies also with polarization:

- In the case of Eq. 3 the coherence depends only on the height of the volume layer and is therefore independent of polarization.
- In Eq. 5 the extinction coefficient can vary with polarization modifying *F(z)* and introducing a dependency of the observed interferometric coherence from polarization. Such volumes with polarization dependent extinction coefficient are called Oriented Volumes (OV) [6].
- In Eq. 7 - apart from the extinction coefficient - the ground-to-volume amplitude ratio *m* is a function of polarization due to the strongly polarized ground scattering component [5].

2.2 Frequency Dependency

Analogously, the variation of *F(z)* with frequency makes the interferometric coherence frequency dependent:

- The model of Eq.3 predicts a frequency independent interferometric coherence as it accounts only for the height of the volume layer.
- The extinction coefficient increases with increasing frequency modifying *F(z)* in Eq. 3, making the interferometric coherence of Eq. 4 frequency dependent. In Fig. 1 the variation of the forest attenuation rate vegetation with frequency (covering a frequency range from about 500MHz (almost P Band) to 5GHz (C Band)) is shown, obtained from experimental data and representative for 20 (lower line), 50 (middle line) and 80% (upper line) of the forest types [7]. Note that the extrapolation towards higher (i.e. X Band) but also lower frequencies is problematic. The maximum volume height that can be estimated is limited by the penetration depth that decreases with increasing extinction. With further increasing height the interferometer do not "see" anymore the whole volume and the height estimation "saturates". Fig. 2 shows the expected penetration depths as function of frequency obtained by using the attenuation rates of Fig. 1. Accordingly the mean (50% line) penetration depth varies from 60m at P Band to 40m at L Band and to 20m at C Band.
- If the volume consists of scatterers with different sizes and orientation distributions the differential extinction (i.e. expressing the change of extinction with polarisation) changes with frequency as the effective scatterers change.
- In the case of combined ground and volume scattering (Eq. 7) in addition to the extinction also the ground scattering amplitude is a function of frequency enforcing the variation of the interferometric coherence with frequency.

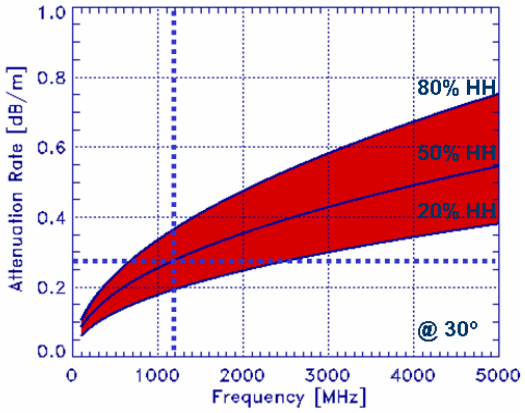

Figure 1 Forest attenuation rate (HH channel at 30° incidence) vs. frequency obtained from the attenuation values in [7] and assuming a vegetation height of 20m.

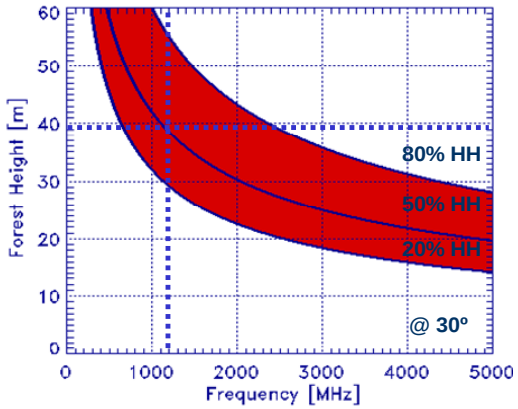

Figure 2 Penetration depth vs. Frequency (for HH at 30° incidence) obtained from the attenuation rates of Fig. 1 and assuming a NESZ of -25dB.

3 Inversion Scenarios

Based on the previous discussion the inversion of forest parameters from polarimetric single- or dual-baseline interferometric data at different frequencies (X, L and P Band) is discussed.

L Band: The inversion of the RVoG model using Pol-InSAR data has been primarily addressed at L-band. In the Quad-pol single-baseline case the inversion problem is balanced with six unknowns ($h_V, \sigma, m_{1-3}, \varphi_0$) and three measured complex coherences [$\tilde{\gamma}(\vec{w}_1) \quad \tilde{\gamma}(\vec{w}_2) \quad \tilde{\gamma}(\vec{w}_3)$] each for any independent polarization channels. However the full inversion [5]

$$\min_{h_V,\sigma,m_i,\varphi_0} \left\| \left[\tilde{\gamma}(\vec{w}_1) \quad \tilde{\gamma}(\vec{w}_2) \quad \tilde{\gamma}(\vec{w}_3)\right]^T - \left[\tilde{\gamma}(h_V,\sigma,m_1) \quad \tilde{\gamma}(h_V,\sigma,m_2) \quad \tilde{\gamma}(h_V,\sigma,m_3)\right]^T \right\|$$

is ambiguous and has to be regularized [8]. With respect to the general L Band scattering scenario, with moderate extinction and relative small m values the approximation that the smallest m is zero has been proved to be efficient [8]

$$\min_{h_V,\sigma,m_i,\varphi_0} \left\| \left[\tilde{\gamma}(\vec{w}_1) \quad \tilde{\gamma}(\vec{w}_2) \quad \tilde{\gamma}(\vec{w}_3)\right]^T - \left[\tilde{\gamma}_V(h_V,\sigma,m_1) \quad \tilde{\gamma}_V(h_V,\sigma,m_2) \quad \tilde{\gamma}_{Vo}\, exp(i\varphi_0)\right]^T \right\|$$

X Band: moving from L Band to X Band - and assuming a close canopy homogeneous forest - the extinction increases attenuating more and more the ground scattering contribution. Furthermore, with increasing extinction the interferometric coherence increases as the effective phase center moves towards the top. The availability of a Quad-pol InSAR system allows the implementation of the L Band inversion scenario (i.e., Eq. 11). However, in this high extinction / low differential extinction / low ground scattering domain the dependency of the interferometric coherence on polarization is rather limited. One possible approximation towards a simplified inversion scenario is to ignore complete the ground scattering component assuming $m=0$ for all polarizations. Using the interferometric coherence at a single polarization channel leads to an underdetermined inversion problem with 3 unknowns and only 1 (complex) observable. Fixing the extinction value allows to obtain a determined problem

$$\min_{h_V,\varphi_0} \left\| \tilde{\gamma}(\vec{w}) - \tilde{\gamma}_V(h_V,\varphi_0 \mid \sigma = \sigma_0) \right\| \qquad -12)$$

that can be further reduced to a single parameter (real) problem if the ground phase is neglected

$$\min_{h_V} \left\| \; |\tilde{\gamma}(\vec{w})| - |\tilde{\gamma}_V(h_V,\varphi_0 \mid \sigma = \sigma_0)| \; \right\| \qquad -13)$$

However, the variance of coherence with polarization can be used as indicator for having reached or not the penetration depth.

P Band: moving from L Band to P Band now the extinction of the vegetation layer decreases, increasing - in general - the ground-to-volume ratio m. Large m_G values in the presence of dihedral scattering - increase further the m level and lead to high interferometric coherences.
In this low extinction / high ground scattering domain polarimetry plays an essential role. The assumption of $m=0$ even for a single polarization is no longer legitimated and can introduce significant estimation errors. A more appropriate regularization at P Band is to fix the extinction value (or even set the extinction to zero) and allow $m \neq 0$ for all polarization channels

$$\min_{h_V,\sigma,m_i,\varphi_0} \left\| \left[\tilde{\gamma}(\vec{w}_1) \quad \tilde{\gamma}(\vec{w}_2) \quad \tilde{\gamma}(\vec{w}_3)\right]^T - \left[\tilde{\gamma}_V(h_V,m_1 \mid \sigma) \quad \tilde{\gamma}_V(h_V,m_2 \mid \sigma) \quad \tilde{\gamma}_V(h_V,m_3 \mid \sigma)\right]^T \right\|$$

However, in the absence of a dihedral scattering component the ground-to-volume ratio m may decreases drastically because of the weak direct ground contribution at P Band. In this case, the same inversion scheme as at L Band (Eq. 11) can be applied.

4 Results and Conclusions

In August 2004 DLR's E-SAR acquired interferometric data at P Band (quad-pol repeat-pass), L Band (quad-pol repeat-pass) and X Band (single-pol single-pass) over the Kobernausser Wald test site in Austria. The terrain of the test site is gently sloped covered by even aged temperate coniferous dominated forest. As reference canopy height data, laser scanner data acquired by the TopoSys sensor (strip length approx. 9 km, horizontal resolution 50 cm and height accuracy 15 cm) consisting of surface height model and digital terrain model have been acquired.
Forest height maps have been inverted from quad-pol single-baseline Pol-InSAR data at L Band and P Band data (using Eq. 11 and 14) and single-pol (VV) single-baseline X Band data (using Eq. 13 and fixing the extinction to 0.5 dB/m). The obtained results are shown in Figure3. As height reference the Lidar H100 is calculated as the maximum height within a 10m by 10m moving window [1]. Comparing the estimated heights out of radar with Lidar one can see that every frequency is able to reconstruct the main forest structures The obtained heights fit the reference Lidar H100 values better (i.e. with a lower variance) at L and P Band and a higher variance at X Band. The overestimation of height at L and P Band can be due to uncompensated decorrelation contributions. At X Band variant extinction values may cause over and underestimation, while the high underestimation in certain areas is due to the limited penetration depth.

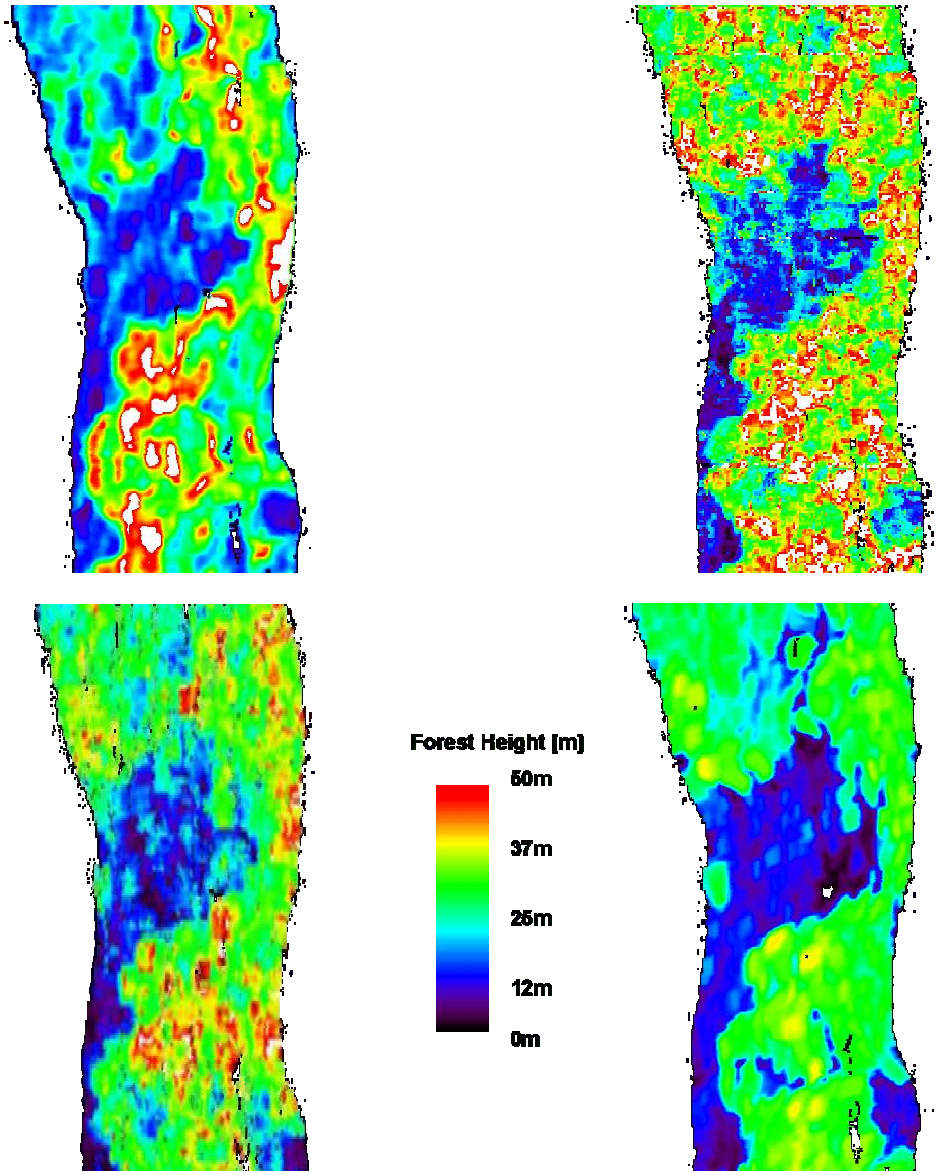

Figure3: Inversion results: Top: X Band (left) and L Band (right). Bottom: P Band (left) and Lidar H100 (right).

References

[1] T., Mette, K.P., Papathanssiou, I., Hajnsek "Potential of forest height derived by Polarimetric SAR Interferometry to estimate forest biomass." Proceedings EUSAR 2004 16 – 18 Mai Ulm

[2] T., Mette, K.P., Papathanssiou, I., Hajnsek, "Estimatin Forest Biomass from Poarimetric Interferometric SAR Data in Combination with Forest Allometry – Results from temperate spruce Forest test site Trausnstein", Proceedings. Retrieval of Bio- and Geophysical Paramters from SAR data for land applications, 16 – 19 November 2004, Innsbruck

[3] R. Bamler, & P. Hartl, "Synthetic Aperture Radar Interferometry", Inverse Problems, vol. 14, pp. R1-R54, 1998.

[4] R.N. Treuhaft, S.N. Madsen, M. Moghaddam, and J.J. van Zyl, "Vegetation Characteristics and Underlying Topography from Interferometric Data", Radio Science, vol. 31, pp. 1449-1495, 1996.

[5] K.P. Papathanassiou and S.R. Cloude, "Single baseline Polarimetric SAR Interferometry'', IEEE Transactions on Geoscience and Remote Sensing, vol. 39, no. 11, pp. 2352-2363, 2001.

[6] R. Treuhaft and S.R. Cloude, "The Structure of Oriented Vegetation from Polarimetric Interferometry", IEEE Transactions on Geoscience and Remote Sensing, vol. 37, no. 5, pp. 2620-2624, 1999.

[7] L. A. Bessette, S Ayasli "Ultra Wide band P-3 and Carabas II Foliage Attenuation and backscatter Analysis", Proceedings of IEEE Radar Conference, pp 357-362, 2001.

[8] S.R. Cloude and K.P., Papathanassiou, "Three-stage inversion process for polarimetric SAR interferometry", IEE Proceedings - Radar Sonar and Navigation, vol. 150, no. 3, pp. 125-134, 2003.